



**HAL**  
open science

## **STARLOC: the star tracking algorithm for the MICADO Lyot coronagraphs**

Elsa Huby, Pierre Baudoz, Fabrice Vidal, Eric Gendron, Yann Clenet, Richard  
Davies

► **To cite this version:**

Elsa Huby, Pierre Baudoz, Fabrice Vidal, Eric Gendron, Yann Clenet, et al.. STARLOC: the star tracking algorithm for the MICADO Lyot coronagraphs. Adaptive Optics for Extremely Large Telescopes 7th Edition, ONERA, Jun 2023, Avignon, France. 10.13009/AO4ELT7-2023-109 . hal-04402896

**HAL Id: hal-04402896**

**<https://hal.science/hal-04402896>**

Submitted on 18 Jan 2024

**HAL** is a multi-disciplinary open access archive for the deposit and dissemination of scientific research documents, whether they are published or not. The documents may come from teaching and research institutions in France or abroad, or from public or private research centers.

L'archive ouverte pluridisciplinaire **HAL**, est destinée au dépôt et à la diffusion de documents scientifiques de niveau recherche, publiés ou non, émanant des établissements d'enseignement et de recherche français ou étrangers, des laboratoires publics ou privés.



## STARLOC: the star tracking algorithm for the MICADO Lyot coronagraphs

Elsa Huby<sup>a</sup>, Pierre Baudoz<sup>a</sup>, Fabrice Vidal<sup>a</sup>, Eric Gendron<sup>a</sup>, Yann Clénet<sup>a</sup>, and Richard Davies<sup>b</sup>

<sup>a</sup>LESIA, Observatoire de Paris, Université PSL, CNRS, Sorbonne Université, Université Paris Cité, Meudon, France

<sup>b</sup>Max-Planck-Institut für extraterrestrische Physik, Garching, Germany

### ABSTRACT

The ELT/MICADO instrument will feature a high contrast mode offering a set of classical Lyot coronagraphs: three different sizes of focal plane occulting spots for optimized observations in the J, H and K spectral bands. Due to the complexity of the instrument and the unprecedented size of its optical elements, star image drift from the coronagraph center is expected during observations, potentially degrading the coronagraph performance. Atmospheric dispersion may not be fully compensated due to the wavelength difference between the AO WFS (visible) and the science camera (IR), and mechanical drift resulting from temperature variations during the night can also induce such drift.

To address these challenges, we have developed the Star Tracking Algorithm for Regular Lyot Occulting Coronagraphs (STARLOC). The aim of STARLOC is to estimate the centering error of the star image onto the occulting spot of the Lyot coronagraph, with the goal of stabilizing the star image within 0.5 mas of the coronagraph center. When the star image is not centered on the occulting Lyot spot, unwanted light leakage occurs, reaching the detector. This leakage can be utilized to estimate the centering error, or tip-tilt aberration.

We explored two approaches to analyze the coronagraphic image: the QACITS approach, originally developed for vortex-type coronagraph and based on the flux asymmetry measurement, and a correlation-based method for monitoring the shift of the coronagraphic image. In this paper, we will report on the comparison of these approaches, in particular in the presence of static aberrations.

**Keywords:** MICADO, high contrast imaging, tip-tilt control, classical Lyot coronagraph

### 1. INTRODUCTION

MICADO will be the first light instrument on the ELT [4], offering a single conjugated adaptive optics system (SCAO [3]). The high contrast mode will include a set of classical Lyot coronagraphs. Three different sizes of focal plane occulting spots will be available to optimize the observations in the J, H and K spectral bands. Their on-sky projected radii will be 15 mas for CLC0, 25 mas for CLC1 and 50 mas for CLC2. For more details, see the related proceeding in this conference[1].

The contrast performance of a coronagraphic instrument is highly dependent on the wavefront quality and stability of the beam incident on the coronagraphic mask. In particular, tip-tilt aberrations induce centering errors onto the focal plane mask and are responsible for stellar light leaking through the coronagraph, thereby degrading the contrast performance. In any type of coronagraph, tip-tilt control is critical to ensure and maintain the contrast performance. Depending on the coronagraph and instrument design, tip-tilt sensors can be implemented as an instrument subsystem, like the differential tip-tilt sensor (DTTS) in the SPHERE instrument[2], or the low-order wavefront sensor (reflective Lyot stop[10]), or directly in the focal plane like the Quadrant Analysis of Coronagraphic Images for Tip-Tilt Sensing (QACITS) method[8].

In the MICADO instrument, a drift of the star image on the coronagraphic image may be induced by differential atmospheric dispersion between the visible wavelength range used by the SCAO visible wavefront sensor (WFS) and the infrared wavelength of the science beam incident on the coronagraph. Temperature variations during the night can also lead to mechanical flexures, which may cause a drift of the star image. As illustrated in Figure 1, simulations of a linear drift over 1 hour show that the central part of the image within a few  $\lambda/D$  will be significantly affected, with the drift becoming the limiting factor above the turbulent AO residuals. Drift rates of less than 0.5 mas per hour are required for the J band while a drift of up to 1 mas per hour may be acceptable in the K band. Given the expected drift rates on the order of a few mas per hour according to the instrument design, a dedicated tip-tilt control system is critical.

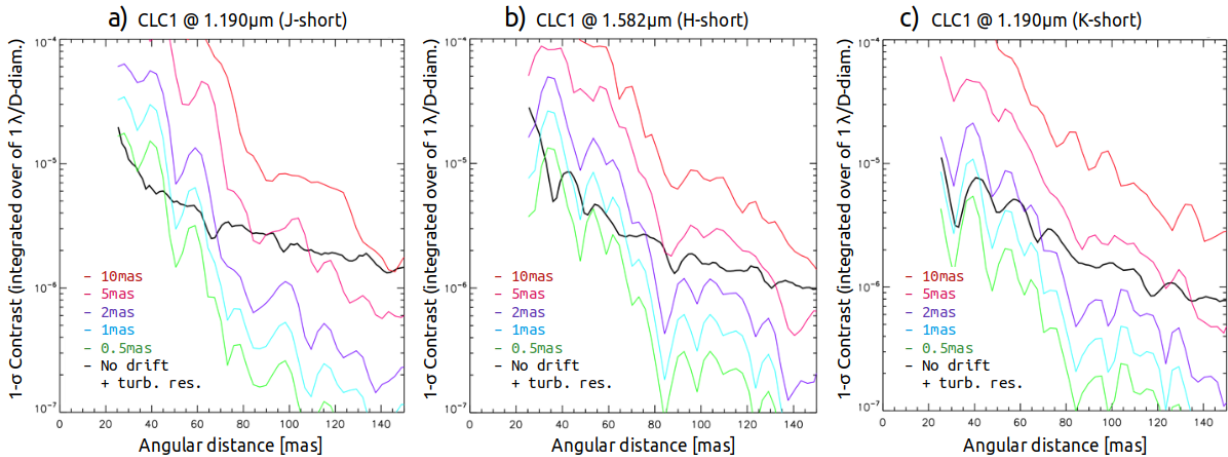


Figure 1. Impact of different tip-tilt drift rates on contrast. For the sake of speed, the contrast curves in the presence of tip-tilt drift are simulated without residual turbulence, while the reference contrast curve includes AO residuals (based on COMPASS simulations[6, 11]). Each simulation represent a 1-hour observation at a zenith angle of  $20^\circ$  with CLC1, processed with classical angular differential imaging. The contrast is defined as the standard deviation computed radially on images convolved by a disk of diameter  $1\lambda/D$  and normalized by the integrated flux of the off-axis PSF at that distance. Panels a, b and c show the results obtained in J, H and K respectively.

The solution based on the analysis of the focal plane image was a natural choice within the MICADO instrument. When the image of the star is not centered onto the coronagraph (i.e., the occulting spot), light leaks through to the detector, which can be used to estimate the centering error, or tip-tilt error. Analyzing the coronagraphic image ensures that there is no non-common path error between the tip-tilt estimate and the actual error, as can occur when the tip-tilt sensor is implemented as a dedicated separate setup, with the beam split upstream of the coronagraphic focal plane. Additionally, the ease of implementation is an advantage in an instrument as complex as MICADO.

In this article, we describe the Star Tracking Algorithm for Regular Lyot Occulting Coronagraph (STARLOC), developed to estimate the centering error affecting the star image on the Lyot occulting mask, based on the analysis of the coronagraphic image. Two approaches were investigated: the QACITS approach and the correlation-based method. The principle of each of them is described in Section 2, while a comparison of their performance in presence of static aberrations is reported in Section 3.

## 2. STARLOC PRINCIPLE

In this section we introduce the principle of the STARLOC loop, how it will be implemented during observations and how the centering error will be estimated.

### 2.1 STARLOC operation

A few steps are needed before running the STARLOC loop, and the currently foreseen acquisition procedure is described as follows and illustrated in Figure 2. Unlike the QACITS technique deployed on the Keck/NIRC2 instrument [7], STARLOC cannot be used as an absolute tip-tilt sensor because of the impact of quasi-static aberrations, which will bias the measurement. STARLOC will instead track and stabilize the star image at a given position chosen as the reference. A reference coronagraphic image has to be defined and measured. The current assumption is that the star will be centered onto the coronagraph mask within 0.5 mas as per the alignment accuracy performed at steps 1 to 3, prior to running the STARLOC loop. The position of the coronagraphic mask center will be estimated beforehand by fitting the position of the occulting spot in a sky background image or internal flat field image, as it is expected to appear as a dark circular area. In addition, an off-axis PSF image is required to normalize the flux in the coronagraphic images, which is necessary for QACITS and possibly for assessing and monitoring the coronagraphic attenuation over time, as well as for photometric calibration purposes during post-processing.

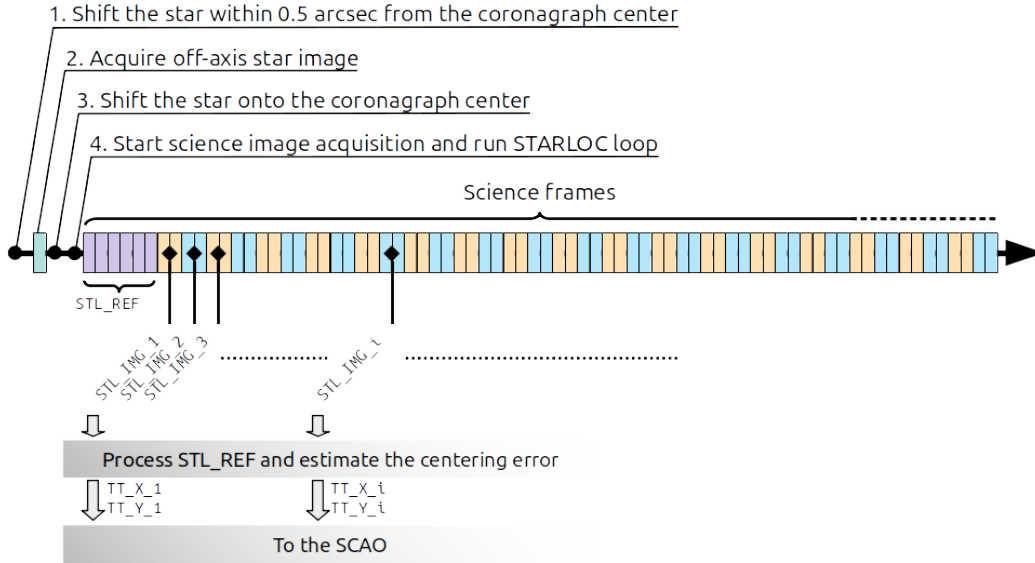


Figure 2. Detailed steps performed during an observation sequence with the MICADO Lyot coronagraph, reported on a timeline. Steps 1 to 3 are performed prior to running the STARLOC algorithm. Each small rectangle represents the acquisition of an image: the off-axis PSF image is the first green rectangle on the left, all the others are science frames. The STARLOC reference frame is computed as the average of the  $NDIT_{REF}$  first science frames (6 in this schematic representation), while subsequent STARLOC frames are computed as the average of  $NDIT_{STL}$  science images (only 2 in this schematic overview).

In the following,  $STL_{REF}$  and  $STL_{IMG}^i$  refer to the STARLOC reference image and the image at the  $i^{\text{th}}$  iteration in the loop, respectively.  $NDIT_{REF}$  and  $NDIT_{STL}$  correspond to the number of science images used to compute  $STL_{REF}$  and  $STL_{IMG}^i$ , respectively.  $DIT_{CORO}$ ,  $DIT_{REF}$ , and  $DIT_{STL}$  define the total integration times for a single science coronagraphic image, the reference STARLOC image, and any STARLOC image, respectively. The sequential steps of the observation procedure with a coronagraph are as follows:

1. Offset the star in the field of view at a position within 0.5 arcsec from the coronagraph mask center.
2. Acquire an off-axis star image cube, which is required for flux normalization. This acquisition is done with one of the three Lyot stops depending on whether a neutral density filter is needed to prevent starlight saturation.

3. Estimate the position of the star image, by fitting its dark-subtracted image by a 2D-Gaussian function, and shift the star image onto the coronagraph mask center. At this point, the star image is assumed to be properly centered onto the coronagraph, within an accuracy 0.5 mas provided by the alignment accuracy.
4. Acquire Science image cubes and run the STARLOC loop in parallel:
  - 4.1. Define the STARLOC reference image,  $STL_{REF}$ , by averaging the first  $NDIT_{REF}$  science images, corresponding to a total integration time of  $DIT_{REF} = NDIT_{REF} * DIT_{CORO}$ .
  - 4.2. Average the next  $NDIT_{STL}$  science images to produce  $STL_{IMG}^i$ , with a total integration time of  $DIT_{STL} = NDIT_{STL} * DIT_{CORO}$ .
  - 4.3. Estimate the centering error.
  - 4.4. Send the error in pixels to the SCAO for correction:  $TT_X^i, TT_Y^i$
  - 4.5. Go to 4.2. and increment  $i$ .

The estimation of the centering error (step 4.3.) will be performed on images computed as the average of a certain number of science frames, depending on the desired correction loop frequency and signal-to-noise ratio in the image. Two analysis methods were explored: the QACITS approach and the correlation-based method.

## 2.2 The QACITS approach

QACITS was originally developed for the vortex-type coronagraph. The flux asymmetry is measured in a selected region, typically an annulus, that is selected to provide a linear model between the flux measurement and the

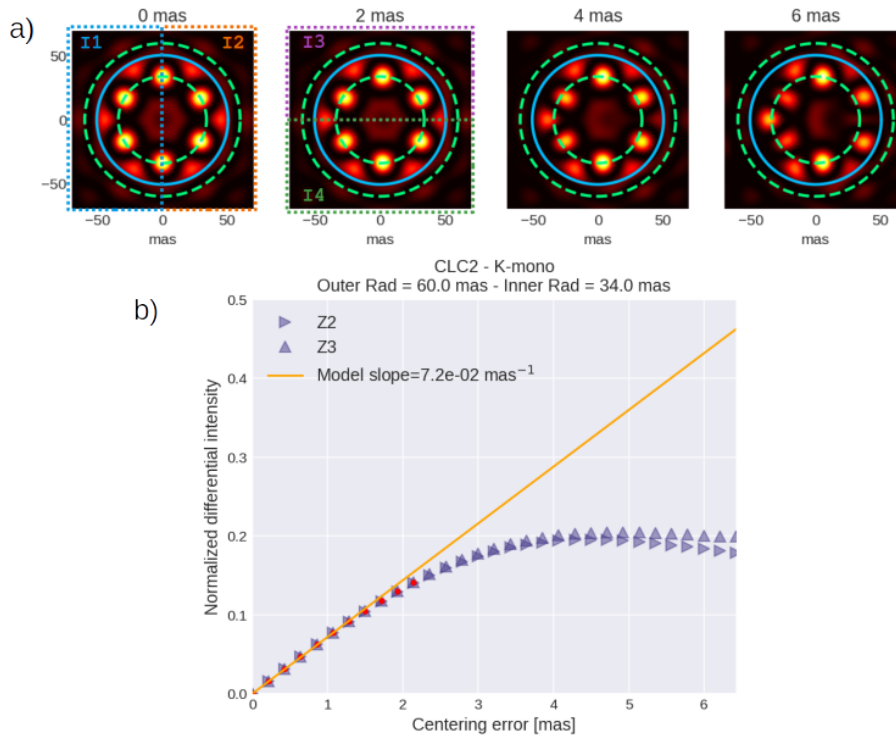


Figure 3. a) Simulated coronagraphic images, for CLC2 (50mas radius) in monochromatic light at 2.145μm. The light blue solid circle shows the edge of the focal plane occulting mask, while the dashed green lines delineate the area used for the QACITS-like analysis (here an annulus between 34 and 60 mas). Rectangles are used to define the quadrants for computing differential intensities in both the horizontal (I2-I1) and vertical (I4-I3) directions. The centering error increases from 0 to 6 mas towards the right, as labeled on top of each image. b) Measurement of the differential intensity with a ramp in Z2 (tip) and Z3 (tilt) within the optimal zone defined for CLC2 in K. A linear fit is performed in the range 0 - 2 mas. For larger centering error, the flux asymmetry deviates from linearity, leading to an underestimation of the true tip-tilt value.

amplitude of the centering error. The asymmetry is quantified based on the flux integrated in four quadrants, similar to a four-quadrant cell, as illustrated in Figure 3-a).

In order to take the magnitude of the star into account, the flux in the coronagraphic image is normalized by dividing it by the flux integrated within a disk of radius  $1.4 \lambda/D$  in the off-axis PSF image, which is acquired at the beginning of the observations sequence (this PSF is also essential for photometric calibration during post-processing). Additionally, a reference image is defined at the start of the acquisition sequence, assuming the star image is correctly centered on the coronagraph center based on the alignment accuracy. This reference image is then subtracted from all subsequent science images analyzed by the QACITS method to mitigate the impact of possible higher order aberrations. The detailed steps of the observation sequence are described in the previous Section.

Similar to the vortex coronagraph case, the relationship between flux asymmetry and the centering error can exhibit a counter-intuitive behavior, where the brightness increases on the left side of the image while the star image is drifting to the right. This effect is illustrated in Figure 3-a) (especially in the very central zone) and its amplitude varies depending on the coronagraph configuration (occluding spot size and wavelength).

The optimal disk or annulus region was determined through the analysis of simulated images with a ramp of centering error. The simulations performed in this study are based on monochromatic light assumption (J:  $1.2475\mu\text{m}$ , H:  $1.635\mu\text{m}$ , or K:  $2.145\mu\text{m}$ ). Given the negligible speckle dispersion due to spectral bandwidth at short distance, the present monochromatic study can be extended to polychromatic images.

The optimal analysis areas were selected by considering several criteria to ensure:

- that the differential intensities in both directions (I2-I1 and I4-I3) exhibit the same variation amplitude (which is not always the case, since the diffraction pattern may slightly differ depending on the tip-tilt direction with respect to the spiders);
- that the differential intensity varies linearly with the centering error, at least for small ranges up to 2 mas;
- the highest possible slope value in the linear model fitted to the simulated data to enhance the sensitivity;
- that the analysis area is kept within the boundaries of the occulter spot of the coronagraph, whenever feasible, preventing an astrophysical signal at very small separation to induce bias into the measurement.

As an example, Figure 3-b) shows the model for CLC2 in K band, based on the selected area between 34 mas and 60 mas, as indicated by the annulus outlined in Figure 3-a). The analysis areas as selected for each coronagraph configuration are displayed in Fig. 4.

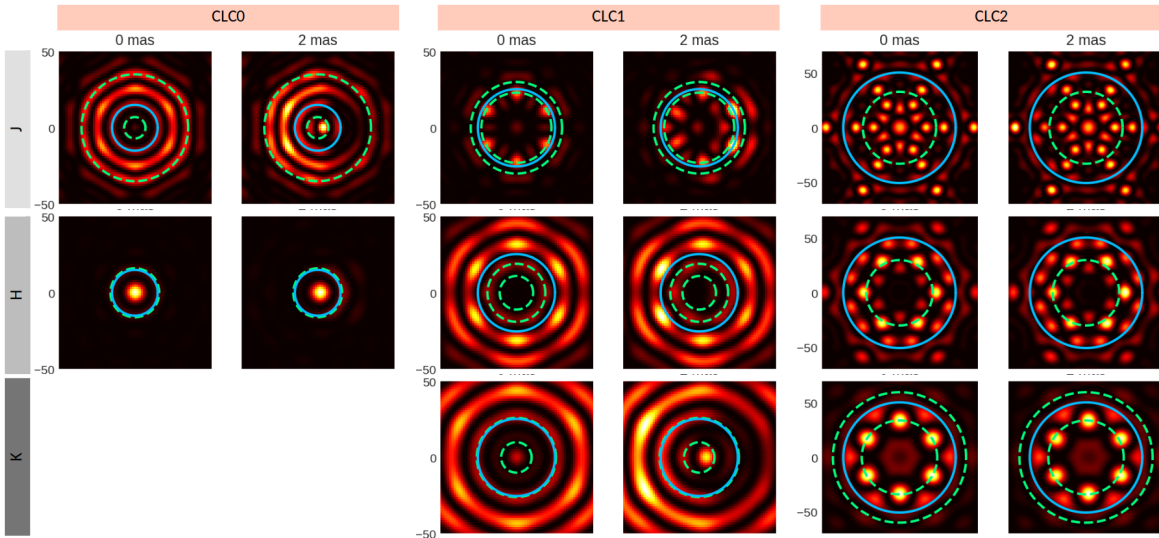


Figure 4. Diffraction patterns obtained for the three coronagraphs in the three different bands (monochromatic light). The solid blue line shows the edge of the occulter mask, while the dashed green lines show the region that is analyzed in the QACITS-like approach.

### 2.3 The correlation-based method

The correlation-based method was proposed based on the idea that, in the presence of a centering error, the coronagraphic image not only changes in shape but also shifts, following the conventional effect of a tip-tilt aberration in image formation. The principle consists of measuring this image shift by computing the 2D-correlation product between the reference image (as described at step 4.1. of the observation sequence detailed in Section 2.1) and any subsequent coronagraphic image to be analyzed for STARLOC. The center of gravity of the correlation product is estimated using a weighted center of gravity function (WCOG)[9], minimizing bias in the estimate.

The simulations, conducted without aberrations in monochromatic light, confirm the assumption that the image is actually shifted. This is observed in a range much wider than  $\pm 2\text{mas}$ . As shown in Figure 5, the flux in the image may change within its structures, but the image's overall shape shifts as expected. The center of gravity calculation is performed on a sub-image, with a width depending on the coronagraph configuration. It is essential to include all main features of the diffraction pattern within this analysis area for efficiency. Future work may include the study to determine the optimal width and shape of this region.

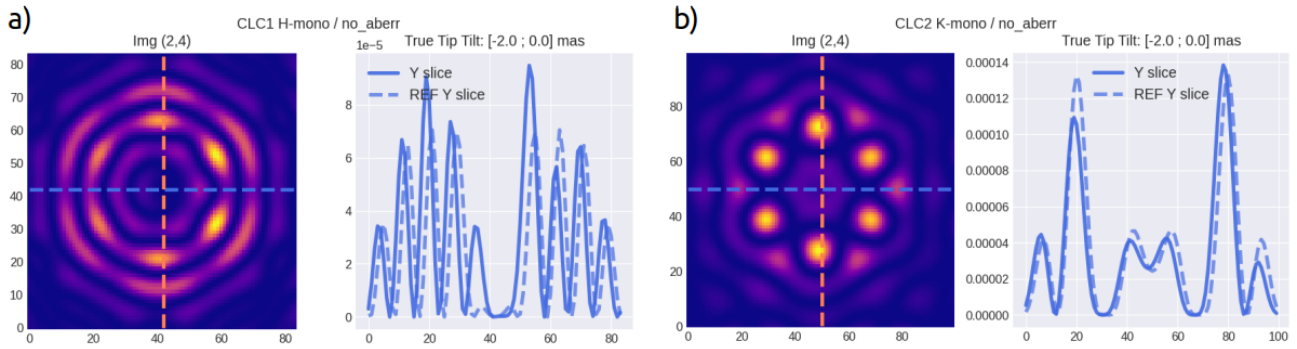


Figure 5. Simulated coronagraphic images, without aberrations, for a) CLC1 in monochromatic H and b) CLC2 in monochromatic K. In both cases there is a centering error of  $-2\text{mas}$  (that is towards the left). The right-hand plots show the horizontal intensity profile cut in the middle, for the reference image (i.e. no centering error, image not shown here) in dashed line and the current image in solid line.

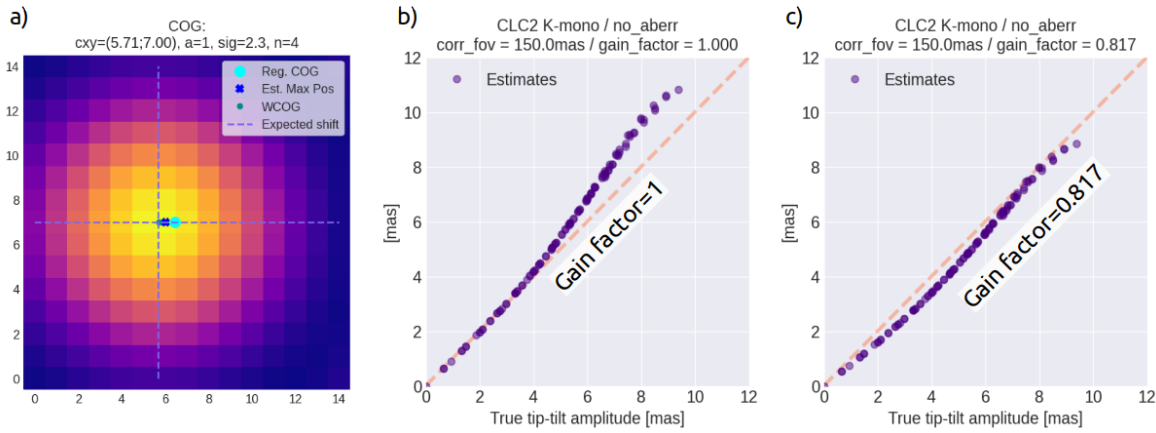


Figure 6. a) Example of a typical correlation product computed from simulated coronagraphic images (without aberrations or noise). Different methods for estimating the position of the maximum of the correlation peak are shown for comparison: position of the maximum (one pixel accuracy), regular COG, weighted COG (WCOG). The true centering error, converted into a fractional number of pixels is indicated by the dashed purple cross. b) An example of correlation-based estimates as a function of the true tip-tilt injected in the simulation. c) Same as b) with a tuned gain factor  $\neq 1$  applied, in order to prevent overestimation of the tip-tilt error.

The implemented center of gravity (COG) function is an iterative process, with the first iteration defined as the position of the maximum pixel in the image. A weighting function centered on this first estimate, with the shape of a supergaussian of order 4 and standard deviation approximately half of the correlation pattern, is then applied before calculating the COG. This process is iterated with the supergaussian function centered on the updated COG estimate, continuing until the estimates do not vary by more than an arbitrary threshold of  $5 \times 10^{-4}$  pixels. This method, originally introduced in the framework of the Shack Hartmann wavefront sensor[9], results in a COG estimate with reduced bias otherwise introduced by the finite size of the correlation window. A comparison between the position of the maximum in the image, the regular COG (without weighting function), and the weighted COG (WCOG) is illustrated in Figure 6-a). The WCOG estimates are then directly converted into units of mas based on the pixel scale (here 1.5 mas/pixel). Overall, the method produces satisfactory results, with a linear range extending well above the 2 mas limit encountered in the QACITS approach, as demonstrated in the example of CLC2 in monochromatic K shown in Figure 6-b). Indeed, figure 6-b) can be directly compared with figure 3-b).

### 3. COMPARISON OF THE TWO METHODS

In order to visualize the efficiency of the centering estimate method, we created a tool that displays the error between the estimate and the true tip-tilt value as a function of the 2D-centering error. For each simulated tip-tilt value  $(t_x, t_y)$ , a vector is drawn to represent the difference between the true and estimated values, with its origin at the true tip-tilt value. This creates a vector field representation, that we call distortion grids. Shorter vectors indicate more accurate estimates. If the vector points toward the center or the outer edge, it signifies that the value is under-estimated or over-estimated, respectively. A gain factor is adjusted to prioritize underestimation over overestimation to prevent over-shooting in a correction loop and divergence, as is illustrated in Figure 6-c). In the QACITS approach this gain factor is tuned by adjusting the slope of the model.

Figure 7-a) and d) display the distortion grids obtained in the ideal case without any aberration or noise, in the example case of the CLC1 coronagraph in monochromatic K light. In both grids, the estimates closely match the true tip-tilt values used in the simulations. The estimates tend to be under-estimated for the largest tip-tilt values. As already highlighted in the previous sections, the linear range is generally broader when using the correlation-based method compared to the QACITS approach (note the graph limits in Figure 7:  $[-2; 2]$ mas for the QACITS approach tests and  $[-4; 4]$ mas for the correlation-based method tests).

A critical condition for the STARLOC algorithm is to work even in the presence of static aberrations arising from non-common path aberrations between the SCAO WFS and the science beam. Two random phase screens representing 80 nm rms phase variations across the aperture were generated, following a power spectral density quadratically decreasing with spatial frequency, which is standard for modeling aberrations introduced by non-perfect optical surfaces [5]. The distortion grids obtained with the two methods are shown in Fig. 7-b-c) for the QACITS approach and e-f) for the correlation-based method. These results highlight the fact that the QACITS approach is significantly impacted by the presence of static aberrations, showing a large discrepancy between the estimated and true tip-tilt values. This means that the flux distribution changes with the centering error, in a way that is not linear anymore. And this impact is largely dependent on the shape of the aberrations, as illustrated by the two grids for the static screen1 and static screen2. In comparison, the grids corresponding to the correlation-based method are also impacted, but with a much smaller magnitude, demonstrating that this method is more robust to the presence of static aberrations.

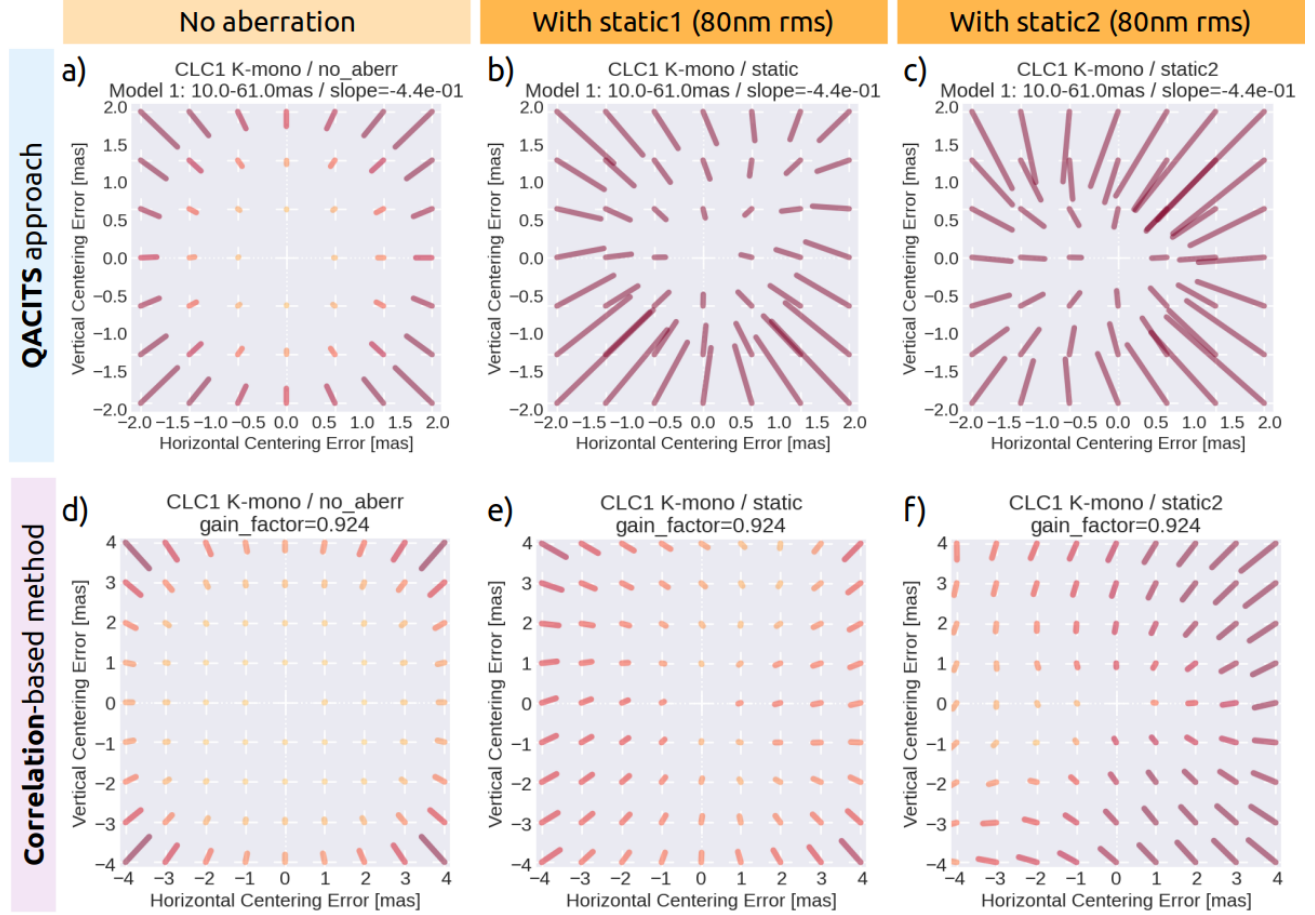


Figure 7. Distortion grids obtained with the CLC1 coronagraph in monochromatic K, using the QACITS-approach to compute the tip-tilt estimates on the top row. The different columns correspond to the following cases: a) no aberration, b) with one static aberration screen (80nm rms) and c) with another static aberration screen (80nm rms). The bottom row displays distortion grids obtained using the correlation-based method for the same aberration cases in d), e), and f), respectively.

#### 4. CONCLUSION

The present work has enabled a comparison of two methods intended for implementation in the STARLOC algorithm, which is designed to track the star image onto the coronagraphic mask in the MICADO instrument. The correlation-based method appears to be more suitable for classical Lyot coronagraphs than the QACITS approach, for several reasons:

- the correlation method has demonstrated greater robustness in the presence of static aberrations;
- the analysis area is a simple square window that captures the main structures of the diffracted light, while the QACITS approach requires finely tuned analysis areas for each coronagraph configuration (occulting spot size + wavelength), sometimes resulting in very thin annuli only a few pixels thick, which can lead to errors due to wrong centering of this analysis area.
- the correlation method provides a linear model on a wider range compared to the QACITS approach, extending up to more than 6 mas for certain coronagraph configurations.

In conclusion, the behavior of the coronagraphic image in presence of tip-tilt aberration is highly dependent on the type of coronagraph. While the correlation-based method proves to be better suited for the classical Lyot coronagraph, quick simulation tests show that it is not adapted to classical vortex coronagraph images, as tip and tilt aberrations are transformed into other aberrations by the phase mask[8].

Following this study, our future investigation will extend to assessing the impact of additional factors, such as photon and read-out noises, turbulent adaptive optics residuals (including jitter), and potential shifts of the Lyot stop. An essential aspect of our ongoing investigation will be the definition of the reference image used to estimate the centering error. Its regular update will be necessary to account for possible changes over time of the static aberrations. To address this, we intend to identify a suitable proxy, potentially involving a combination of the two analysis methods presented here and/or monitoring of starlight attenuation, to determine when the reference image is no longer valid and needs to be updated.

## ACKNOWLEDGMENTS

This work was supported by the Action Spécifique Haute Résolution Angulaire (ASHRA) of CNRS/INSU co-funded by CNES.

## References

- [1] Pierre Baudoz et al. “Design and performance of MICADO high contrast mode”. In: *Proceedings of AO4ELT7*. 2023.
- [2] Pierre Baudoz et al. “The differential tip-tilt sensor of SPHERE”. In: *Ground-based and Airborne Instrumentation for Astronomy III*. Ed. by Ian S. McLean, Suzanne K. Ramsay, and Hideki Takami. Vol. 7735. Society of Photo-Optical Instrumentation Engineers (SPIE) Conference Series. July 2010, 77355B, 77355B. DOI: [10.1117/12.858274](https://doi.org/10.1117/12.858274).
- [3] Yann Clenet et al. “MICADO SCAO: to be or not to be... in MAIT”. In: *Proceedings of AO4ELT7*. 2023.
- [4] Richard Davies et al. “MICADO: the E-ELT adaptive optics imaging camera”. In: *Ground-based and Airborne Instrumentation for Astronomy III*. Ed. by Ian S. McLean, Suzanne K. Ramsay, and Hideki Takami. Vol. 7735. Society of Photo-Optical Instrumentation Engineers (SPIE) Conference Series. July 2010, 77352A, 77352A. DOI: [10.1117/12.856379](https://doi.org/10.1117/12.856379). arXiv: [1005.5009](https://arxiv.org/abs/1005.5009) [[astro-ph.IM](https://arxiv.org/abs/1005.5009)].
- [5] Kjetil Dohlen et al. “SPHERE: Confronting in-lab performance with system analysis predictions”. In: *Second International Conference on Adaptive Optics for Extremely Large Telescopes*. Sept. 2011, 75, p. 75.
- [6] D. Gratadour et al. “COMPASS: an efficient, scalable and versatile numerical platform for the development of ELT AO systems”. In: *Adaptive Optics Systems IV*. Ed. by Enrico Marchetti, Laird M. Close, and Jean-Pierre Vran. Vol. 9148. Society of Photo-Optical Instrumentation Engineers (SPIE) Conference Series. Aug. 2014, 91486O, 91486O. DOI: [10.1117/12.2056358](https://doi.org/10.1117/12.2056358).
- [7] E. Huby et al. “On-sky performance of the QACITS pointing control technique with the Keck/NIRC2 vortex coronagraph”. In: *A&A* 600, A46 (Apr. 2017), A46. DOI: [10.1051/0004-6361/201630232](https://doi.org/10.1051/0004-6361/201630232). arXiv: [1701.06397](https://arxiv.org/abs/1701.06397) [[astro-ph.IM](https://arxiv.org/abs/1701.06397)].
- [8] E. Huby et al. “Post-coronagraphic tip-tilt sensing for vortex phase masks: The QACITS technique”. In: *A&A* 584, A74 (Dec. 2015), A74. DOI: [10.1051/0004-6361/201527102](https://doi.org/10.1051/0004-6361/201527102). arXiv: [1509.06158](https://arxiv.org/abs/1509.06158) [[astro-ph.IM](https://arxiv.org/abs/1509.06158)].
- [9] Magalie Nicolle et al. “Optimization of star-oriented and layer-oriented wavefront sensing concepts for ground layer adaptive optics”. In: *J. Opt. Soc. Am. A* 23.9 (Sept. 2006), pp. 2233–2245. DOI: [10.1364/JOSAA.23.002233](https://doi.org/10.1364/JOSAA.23.002233). URL: <https://opg.optica.org/josaa/abstract.cfm?URI=josaa-23-9-2233>.
- [10] Garima Singh et al. “Lyot-based Low Order Wavefront Sensor for Phase-mask Coronagraphs: Principle, Simulations and Laboratory Experiments”. In: *PASP* 126.940 (June 2014), p. 586. DOI: [10.1086/677048](https://doi.org/10.1086/677048). arXiv: [1404.7201](https://arxiv.org/abs/1404.7201) [[astro-ph.IM](https://arxiv.org/abs/1404.7201)].
- [11] Fabrice Vidal et al. “End-to-End simulations for the MICADO-MAORY SCAO mode”. In: *Proceedings of Adaptive Optics for Extremely Large Telescopes (AO4ELT5)*. Apr. 2018, 43, p. 43. DOI: [10.26698/AO4ELT5.0043](https://doi.org/10.26698/AO4ELT5.0043).